Tetrahedron: *Asymmetry* 19 (2008) 1617–1621

Contents lists available at ScienceDirect

Tetrahedron: *Asymmetry*

journal homepage: www.elsevier.com/locate/tetasy

Density functional theory study of the stereoselectivity in small peptide-catalyzed intermolecular aldol reactions

Peter Hammar [a], Armando Córdova [b,*], Fahmi Himo [a,*]

[a] *Department of Theoretical Chemistry, School of Biotechnology, The Royal Institute of Technology, SE-106 91 Stockholm, Sweden*
[b] *Department of Organic Chemistry, Arrhenius Laboratory, Stockholm University, SE-106 91 Stockholm, Sweden*

ARTICLE INFO

Article history:
Received 14 May 2008
Accepted 13 June 2008
Available online 14 July 2008

ABSTRACT

The origins of the stereoselection of the dipeptide-catalyzed intermolecular aldol reaction are explored by means of hybrid density functional theory. Transition states were located for the (*S*)-ala-(*S*)-ala-catalyzed aldol reaction with cyclohexanone as the donor and benzaldehyde as the acceptor. The calculations reproduce the experimental trends very satisfactorily. It is demonstrated that the main source of stereoselectivity is the interaction of the N-terminal amino acid side chain of the dipeptide with the cyclohexene ring.

1. Introduction

The asymmetric aldol reaction is an important C–C bond-forming reaction in synthetic chemistry[1] and in Nature.[2] The enzyme-catalyzed stereoselective aldol reaction involves enamine intermediates (Type I aldolases) or zinc enolates (Type II aldolases) as the reactive nucleophile.[2] The catalytic residue of Type I aldolases is the primary amino group of a lysine residue, which forms enamine intermediates with the help of a proton relay system by neighboring amino acids.[2c] Amino acids and small peptides have also been suggested as ancient catalysts for the asymmetric aldol reaction.[3]

In the 1970s, Hajos and Parrish and Eder et al.,[4,5] discovered that amino acids are able to catalyze the asymmetric aldol reaction via a catalytic enamine mechanism. Their stereoselective Robinson annulations have been utilized numerous times in natural product synthesis.[6] For example, Danishefsky and Cain utilized phenylalanine (1.2 equiv of amino acid) for the synthesis of optically active estrone and 19-norsteroids.[6a] However, it was not until 2000 when List et al. demonstrated that proline and its derivatives are highly enantioselective catalysts for the intermolecular asymmetric aldol reaction between ketones and aldehydes that asymmetric enamine catalysis received increased attention.[7,8] The generally accepted mechanism is that both the proline-catalyzed intramolecular and intermolecular aldol reactions involve an enamine mechanism where one proline molecule takes part in the transition state as suggested by Houk and List.[9] Seebach and Eschenmoser et al. have recently proposed an alternative view of the role of oxazolidinones for the mechanism of this reaction.[10]

Most of the work on the organocatalytic intermolecular aldol reaction involved the use of proline and its derivatives. In 2005, Córdova et al. showed that amino acids with a primary amino functionality are able to catalyze the asymmetric intermolecular aldol reaction with high stereoselectivity.[3b,11] The origins of the stereoselectivity for this reaction were investigated using density functional theory (DFT) calculations.[12] Since these findings, linear amino acids are used more often as catalysts for highly enantioselective intermolecular aldol reactions.[13] Córdova et al. subsequently found that small di- to tetra-peptides with a primary amine functionality also catalyzed the asymmetric intermolecular aldol reaction with excellent enantioselectivity.[14] In addition, the small peptides can catalyze the aldol reaction in water and aqueous media with high asymmetric induction (Eq. 1).[14b] In stark contrast, the parent amino acids are less efficient and furnished nearly racemic products (Eq. 2). These results are of synthetic importance and may have implications for the evolution of homochirality.[14,15]

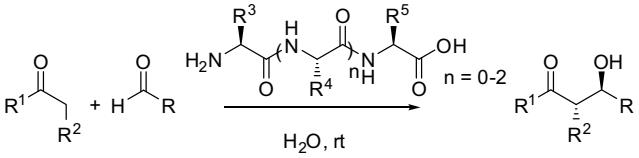

(1)

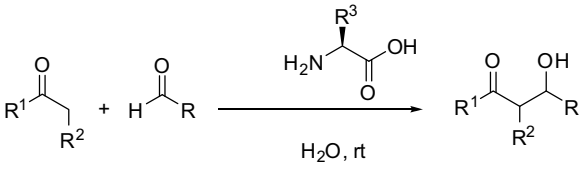

(2)

* Corresponding authors. Fax: +46 855378590 (F.H.).
E-mail addresses: acordova@organ.su.se (A. Córdova), himo@teochem.kth.se (F. Himo).

0957-4166/$ - see front matter © 2008 Elsevier Ltd. All rights reserved.
doi:10.1016/j.tetasy.2008.06.014

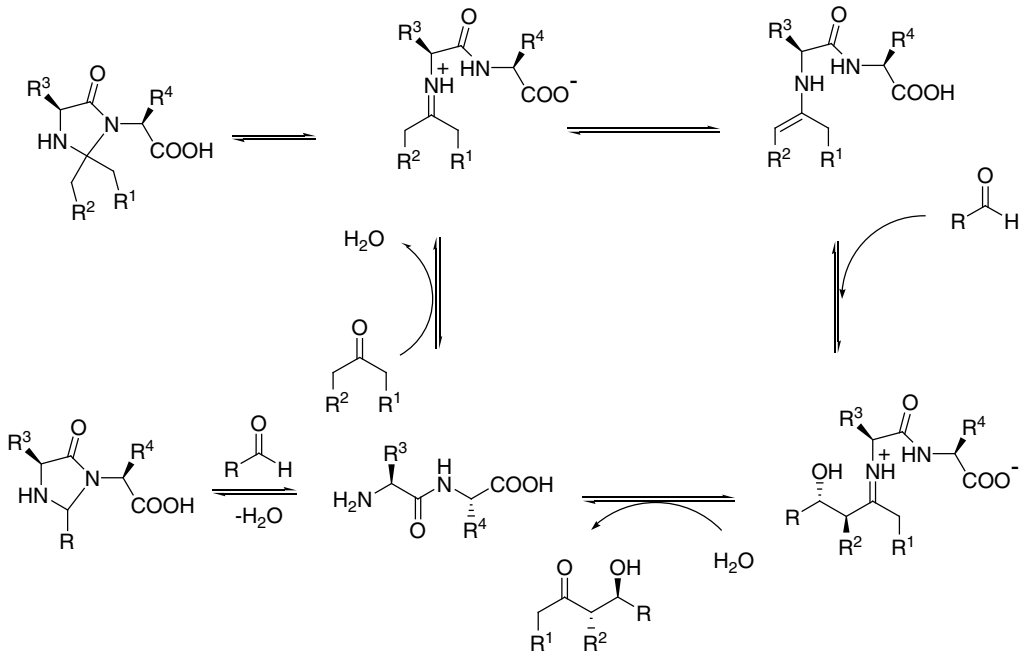

Scheme 1. Proposed reaction mechanism of the dipeptide-catalyzed aldol reaction.

Notably, it was found in vitro that small peptides isolated from living cells can catalyze the asymmetric aldol reaction, demonstrating that non-enzymatic enantioselective catalysis can occur in living cells and be of biological relevance.[14b] For example, the aldol products from these reactions can subsequently undergo Amadori rearrangement that leads to non-enzymatic glycation of amino acids, peptides and proteins (the Maillard reaction).[16,14b] In fact, the Maillard reaction has been implicated in a number of pathologies, such as diabetes mellitus, neurodegenerative amyloid diseases, and normal processes of aging.[16,17]

The suggested acid-mediated enamine mechanism of the dipeptide-catalyzed asymmetric intermolecular aldol reaction is shown in Scheme 1. The ketone donor reacts with the dipeptide via an iminium species to form an enamine intermediate. Next, the acceptor aldehyde reacts with the chiral enamine to give, after hydrolysis, the enantiomerically enriched aldol product; the catalytic cycle can be repeated.

The beneficial effect of water in the small peptide-catalyzed asymmetric aldol reaction has been reported to be due to the improved catalyst turnover via faster hydrolysis of the intermediates of the enamine catalytic cycle, as well as the suppression of catalyst inhibition by non-productive imidazolidinone formation.[14]

Herein, we report the origins of the stereoselectivity of the intermolecular aldol reaction catalyzed by a dipeptide. Density functional theory calculations are used to optimize the transition states of the C–C bond formation step. The calculations accurately predict the stereochemistry of the observed product and provide key insights into the factors governing the enantioselection.

2. Computational details

All the calculations were performed using the hybrid density functional theory method B3LYP[18] as implemented in the GAUSSIAN03 software package.[19] The geometries were optimized using the standard double zeta plus polarization basis set 6-31G(d,p). Based on these geometries, more accurate energies were obtained by performing single point calculations using the much larger 6-311+G(2d,2p) basis set.

Frequency calculations were performed at the same theory level as the optimizations to obtain zero-point energies (ZPE) and to confirm the nature of the stationary points. The latter implies no negative eigenvalues for minima and only one negative eigenvalue for transition states.

Solvation effects were calculated using the CPCM polarizable conductor calculation model ($\varepsilon = 36.6$).[20] The radii derived from the UFF force field were employed to build the cavity.

3. Results and discussion

To investigate the stereochemistry of the dipeptide-catalyzed intermolecular aldol reaction, we chose as a model to study the (*S*)-ala-(*S*)-ala-catalyzed aldol reaction with cyclohexanone **1** as the donor and benzaldehyde **2** as the acceptor which gives the corresponding aldol product **3** (Eq. 3). More specifically, we focused our attention on the nucleophilic attack of the chiral enamine at the carbonyl group, since the stereochemistry of the product is controlled in this step.

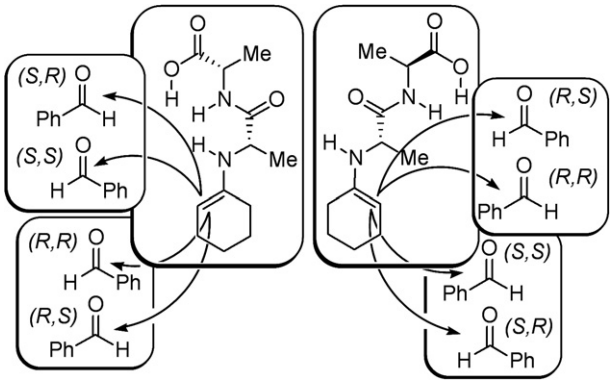

Scheme 2. Arrangements of modes of attack that generate different stereoisomers in the dipeptide-catalyzed aldol reaction between cyclohexanone and benzaldehyde. Left *anti*-enamine and right *syn*-enamine.

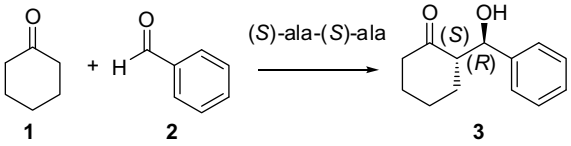

(3)

The reaction of cyclohexanone and benzaldehyde leads to the formation of two stereogenic centers, resulting in four possible stereoisomers (Scheme 2). The enamine can be in either *syn*- or *anti*-conformations, while the enamine can attack from its *Si* or *Re* face on the *Si* or *Re* face of the aldehyde, giving rise to eight different transition states. In addition, for each of these transition states, the enamine and the aldehyde can approach each other in three different staggered fashions, resulting in three rotameric transition states. On top of that, the conformational flexibility of the peptide dramatically increases the number of possible transition state geometries. In total, there are hence a large number of transition states to be considered computationally.

We first focused on the transition states that led to the major product observed experimentally, namely the (2*S*,3*R*)-β-hydroxy ketone **3**. A large number of transition state structures were optimized for this product (10 of them are shown in Figure 1).

The energetically most accessible transition state, TS-(*S*,*R*)-**1**, has several features that make it to have lower energy than all other ones. The conformation of the peptide is optimal in order to form a hydrogen bond between the peptide amide and the

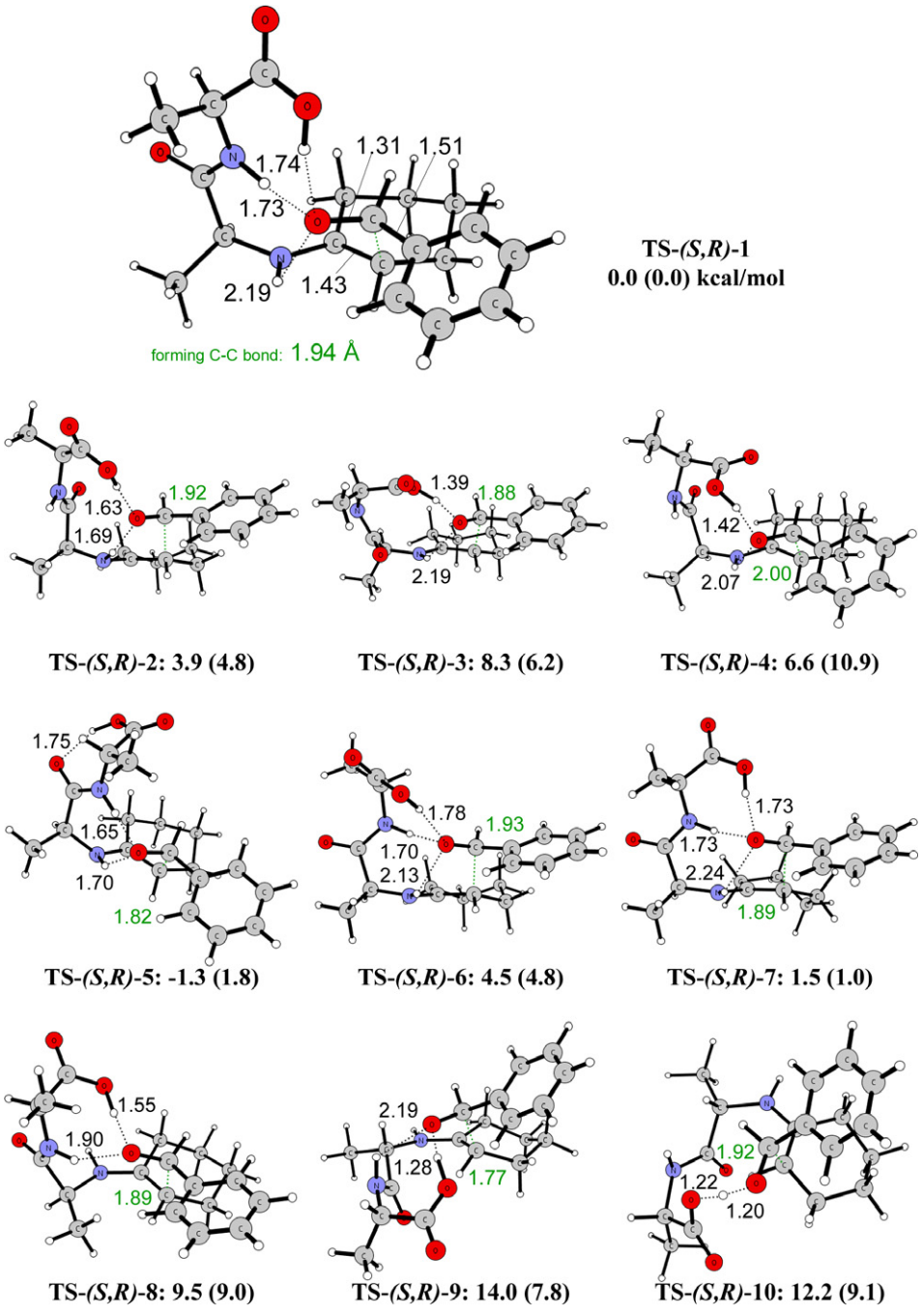

Figure 1. Optimized transition states leading to the (*S*,*R*)-product. Distances are given in Å. Below each figure are the gas phase relative energies in kcal/mol (values including solvation are in parentheses).

alkoxide anion that is developing on the aldehyde. The carboxylic moiety is also in an optimal position to donate its proton. In addition, the developing anion of the aldehyde interacts favorably with the NH moiety of the enamine. These three interactions stabilize the alkoxide anion to a very high degree, making the concerted carbon–carbon bond formation and proton transfer from the carboxyl group very asynchronous, with the proton transfer being much later than the C–C bond formation. Furthermore, the two methyl substituents of the ala-ala dipeptide are pointing away from the substrates and at the same time avoiding steric repulsion from the peptide backbone.

The stabilization of the transition state provided by the three hydrogen bonding interactions is likely one of the main reasons that enable the small peptide to catalyze the intermolecular aldol reaction with high enantioselectivity under aqueous conditions, while the parent amino acid, for which the transition state lacks the hydrogen bonding to the peptide bond, catalyzes the formation of the nearly racemic compounds under the same conditions.[14,15]

Taken together, the features discussed above jointly make the TS-(*S*,*R*)-**1** the most stable one. In all the other transition states, one or several of these features are disturbed (a number of TS structures that lead to the same product are shown in Figure 1).

Any rotation of the peptide chain leading to the loss of hydrogen bonds results in higher barriers. For example, in TS-(*S*,*R*)-**2**, TS-(*S*,*R*)-**3**, and TS-(*S*,*R*)-**4**, the peptide bond is rotated away from the aldehyde, which results in barriers that are 4.8, 6.2, and 10.9 kcal/mol higher than TS-(*S*,*R*)-**1**, respectively. In TS-(*S*,*R*)-**5**, the carboxylic group is pointing away from the aldehyde and instead a hydrogen bond to the carbonyl oxygen of the peptide bond is formed. This results in a barrier that is 1.8 kcal/mol higher than TS-(*S*,*R*)-**1**. In fact, the gas phase energy of TS-(*S*,*R*)-**5** is 1.3 kcal/mol *lower* than that of TS-(*S*,*R*)-**1**, which is a consequence of the gas phase overestimation of the energy contribution of the hydrogen bond between the carboxyl and the peptide carbonyl.

The TS in which all three interactions are conserved, but where the peptide is rotated such that there is a steric repulsion between the methyl side chain of the alanine and the carbonyl of the peptide bond, TS-(*S*,*R*)-**6**, is 4.8 kcal/mol higher than TS-(*S*,*R*)-**1**. The transition state in which the cyclohexene ring adopts a boat conformation TS-(*S*,*R*)-**7** is higher by 1.0 kcal/mol.

When the enamine is in the *syn*-conformation, the transition states leading to the (*S*,*R*) product are all lacking the interaction between the enamine NH and the alkoxide of the aldehyde, resulting in higher energies, see TS-(*S*,*R*)-**8**, TS-(*S*,*R*)-**9**, and TS-(*S*,*R*)-**10** in Figure 1. In these transition states, other effects that contribute to the higher energy are seen. For example, the hydrogen bonds to the peptide NH and the carboxyl are not optimal, and steric repulsion between the methyl group of alanine and the cyclohexene ring, and ring–ring repulsion are seen. These effects lead to energies that are considerably higher than those for TS-(*S*,*R*)-**1**.

In summary, a number of steric and hydrogen bonding interactions make TS-(*S*,*R*)-**1** the optimal transition state, having a lower energy than the other transition states leading to the same product.

We have conducted similar analyses for the transition states leading to the other product isomers. In Figure 2, we present the optimized lowest-energy transition states for each category. Indeed, in agreement with the experimental findings, all other TSs have higher energies compared to TS-(*S*,*R*)-**1**.

For the transition states leading to the (*R*,*S*) product, two transition states were found to have very similar energies [TS-(*R*,*S*)-**1** and TS-(*R*,*S*)-**2**, see Fig. 2], both lying at 3.5 kcal/mol higher energy than TS-(*S*,*R*)-**1**. In TS-(*R*,*S*)-**1**, the three favorable interactions of the developing alkoxide with the carboxylic acid, the peptide bond NH group, and the enamine NH are very similar to the ones found for (*S*,*R*)-**1**. However, to accommodate these interactions in an optimal way, the peptide backbone is rotated such that the methyl substituent of the alanine experiences steric repulsion from both the cyclohexene ring and the carbonyl of the peptide bond. This causes the higher energy and is thus the source of enantioselectivity.

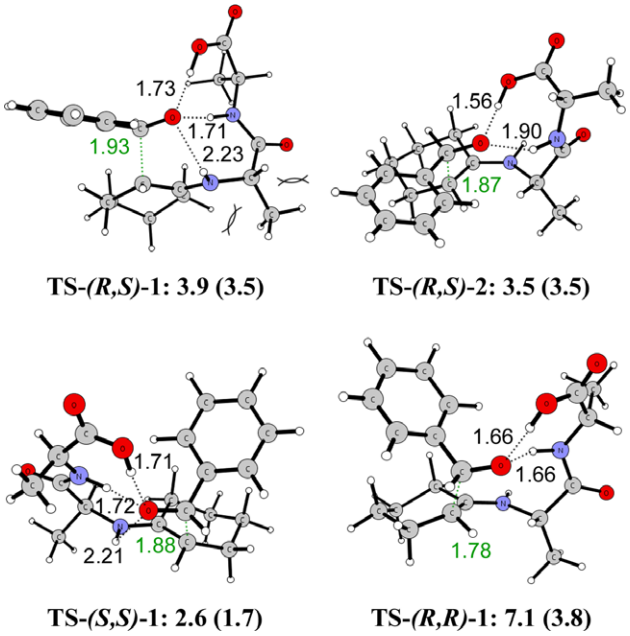

Figure 2. Optimized lowest-energy transition states leading to the minor products. Energies are given relative to TS-(*S*,*R*)-**1** (see Fig. 1). Values including solvation are in parentheses.

In the *syn*-enamine version of this transition state, TS-(*R*,*S*)-**2**, it is possible to avoid this steric repulsion, but this comes at the price of losing the interaction to the enamine proton, which results in a very similar energy.

The lowest transition state leading to the (*S*,*S*)-enantiomer of product (TS-(*S*,*S*)-**1**, Fig. 2) has an energy of 1.7 kcal/mol higher than (*R*,*S*)-**1**. The three favorable interactions of the alkoxide are conserved. However, changing the face of the aldehyde causes a ring–ring repulsion that raises the energy.

Finally, in the lowest transition state leading to the (*R*,*R*)-product TS-(*R*,*R*)-**1** (Fig. 2), two effects are responsible for raising the energy by 3.8 kcal/mol compared to TS-(*S*,*R*)-**1**. These are the lack of interaction with the enamine NH and the ring–ring repulsion.

The relative energies of the lowest-energy transition states leading to the four different stereoisomers are 0.0, 3.5, 1.7, and 3.8 kcal/mol for (*S*,*R*), (*R*,*S*), (*S*,*S*), and (*R*,*R*) enantiomers, respectively. Experimentally, the (*S*,*R*)-product was found to be the major product, with an enantiomeric excess of 91%, which translates

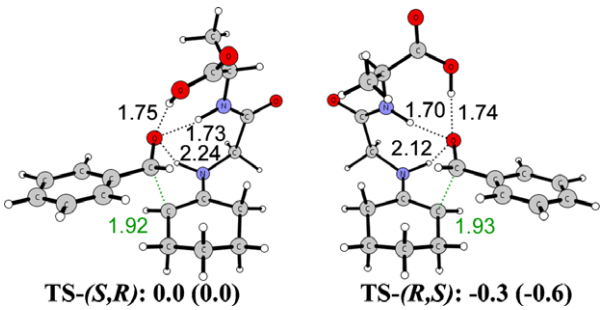

Figure 3. Optimized transition states for the gly-(*S*)-ala catalyst. Relative energies are indicated (values including solvation are in parentheses).

approximately to an energy difference of 1.8 kcal/mol between the (*S*,*R*) and (*R*,*S*) transition states. Our calculated value of 3.5 kcal/mol is thus consistent with the experiment, but somewhat overestimated. Similar overestimation was previously observed for the amino acid-catalyzed aldol reaction.[9h,12]

The experimentally determined diastereomeric ratio (dr) of 8:1 can similarly be converted to an energy difference of about 1.3 kcal/mol. Our calculated energy difference of 1.7 kcal/mol between the (*S*,*R*) and (*S*,*S*) transition states is in good agreement with the experimental value, although also slightly overestimated.

As discussed above, the main source of stereoselectivity is found to be the interaction of the amino acid side chain with the cyclohexene ring. To test this, we changed the methyl group into a hydrogen [effectively changing the catalyst to gly-(*S*)-ala] and reoptimized the TS-(*S*,*R*)-**1** and TS-(*R*,*S*)-**1** transition states (see Fig. 3). The energy difference drops from 3.5 to −0.6 kcal/mol [i.e., TS-(*R*,*S*)-**1** is 0.6 kcal/mol lower than TS-(*S*,*R*)-**1**], making the two transition states almost degenerate. This is in line with the very small ee found experimentally for the gly-(*S*)-ala catalyst (11%).[15a]

4. Conclusion

In the present contribution, we have studied the C–C bond-forming transition state in the (*S*)-ala-(*S*)-ala-catalyzed intermolecular aldol reaction. By calculating a large number of transition states, we were able to analyze, in detail, the factors governing the stereoselectivity. The calculations reproduce very satisfactorily the experimentally determined diastereo- and enantioselectivities.

It is shown that the methyl substituent of the N-terminal alanine causes the transition state leading to the (*R*,*S*)-enantiomer of the aldol product to be higher in energy, mainly by steric repulsion to the cyclohexene ring and the peptide bond. The stabilization of the most favored transition state by three hydrogen bonding interactions is the most likely cause for the ability of the small peptide to catalyze the intermolecular aldol reaction with high enantioselectivity in aqueous conditions, while the parent amino acid catalyzes the formation of nearly racemic compounds under the same conditions.

Acknowledgments

F.H. and A.C. gratefully acknowledge the Swedish National Research Council, Lars Hierta Foundation, the Carl Trygger Foundation, Magn Bergvall Foundation, and the Wenner-Gren Foundations for financial support.

References

1. Trost, B. M.; Fleming, I.; Heathcock, C.-H. In *Comprehensive Organic Synthesis*; Pergamon: Oxford, 1991; Vol. 2; *Modern Aldol Reactions*; Mahrwald, R., Ed.; Wiley-VCH: Weinheim, 2004; Vols. 1 & 2, Carreira, E. M. In *Comprehensive Asymmetric Catalysis*; Jacobsen, E. N., Pfaltz, A., Yamamoto, H., Eds.; Springer: Heidelberg, 1999; Johnson, J. S.; Evans, D. A. *Acc. Chem. Res.* **2000**, *33*, 325; Palomo, C.; Oiarbide, M.; García, J. M. *Chem. Soc. Rev.* **2004**, *33*, 65.
2. (a) Fessner, W.-D. In *Stereoselective Biocatalysis*; Patel, R. N., Ed.; Marcel Dekker: New York, 2000; p 239; (b) Machajewski, T. D.; Wong, C.-H. *Angew. Chem., Int. Ed.* **2000**, *39*, 1352; (c) Heine, A.; DeSantis, G.; Luz, J. G.; Mitchell, M.; Wong, C.-H.; Wilson, I. A. *Science* **2001**, *294*, 369.
3. (a) Pizzarello, S.; Weber, A. L. *Science* **2004**, *303*, 1151; (b) Córdova, A.; Ibrahem, I.; Casas, J.; Sundén, H.; Engqvist, M.; Reyes, E. *Chem. Eur. J.* **2005**, *11*, 4772; (c) Córdova, A.; Engqvist, M.; Ibrahem, I.; Casas, J.; Sundén, H. *Chem. Commun.* **2005**, 2047; (d) Kofoed, J.; Machuqueiro, M.; Reymond, J.-L.; Darbre, T. *Chem. Commun.* **2004**, *26*, 1540.
4. (a) Hajos, Z. G.; Parrish, D. R. German Patent DE 2102623, July 29, 1971; (b) Hajos, Z. G.; Parrish, D. R. *J. Org. Chem.* **1974**, *39*, 1615.
5. (a) Eder, U.; Sauer, G.; Wiechert, R. German Patent DE 2014757, October 7, 1971; (b) Eder, U.; Sauer, G.; Wiechert, R. *Angew. Chem., Int. Ed. Engl.* **1971**, *10*, 496.
6. (a) Danishefsky, S.; Cain, P. *J. Am. Chem. Soc.* **1975**, *97*, 5282; (b) Shimizu, I.; Naito, Y.; Tsuji, J. *Tetrahedron Lett.* **1980**, *21*, 4975; (c) Hagiwara, H.; Uda, H. *J. Org. Chem.* **1988**, *53*, 2308; (d) Corey, E. J.; Virgil, S. C. *J. Am. Chem. Soc.* **1990**, *112*, 6429.
7. (a) List, B.; Lerner, R. A.; Barbas, C. F., III. *J. Am. Chem. Soc.* **2000**, *122*, 2395; (b) Notz, W.; List, B. *J. Am. Chem. Soc.* **2000**, *122*, 7386; (c) Mukherjee, S.; Yang, J. W.; Hoffmann, S.; List, B. *Chem. Rev.* **2007**, *107*, 5471.
8. For selected early contributions on the proline-catalyzed intermolecular aldol reaction see reviews: (a) Dalko, P. I.; Moisan, L. *Angew. Chem., Int. Ed.* **2001**, *40*, 3726; (b) List, B. *Tetrahedron* **2002**, *58*, 5573; (c) Dalko, P. I.; Moisan, L. *Angew. Chem., Int. Ed.* **2004**, *43*, 5138; See also some selected early papers: (d) List, B.; Pojarliev, P.; Castello, C. *Org. Lett.* **2001**, *3*, 573; (e) Sakthivel, K. S.; Notz, W.; Bui, T., ; Barbas, C. F., III. *J. Am. Chem. Soc.* **2001**, *123*, 5260; (f) Córdova, A.; Notz, W.; Barbas, C. F., III. *Chem. Commun.* **2002**, *67*, 3034; (g) Córdova, A.; Notz, W.; Barbas, C. F., III. *J. Org. Chem.* **2002**, *67*, 301; (h) Northrup, A. B.; MacMillan, D. W. C. *J. Am. Chem. Soc.* **2002**, *124*, 6798; (i) Bøgevig, A.; Kumaragurubaran, N.; Jørgensen, K. A. *Chem. Commun.* **2002**, 620; (j) List, B.; Hoang, L.; Martin, H. J. *Proc. Natl. Acad. Sci. U.S.A.* **2004**, *101*, 5839; (k) Nyberg, A. I.; Usano, A.; Pihko, P. *Synlett* **2004**, 1891.; For examples of N-terminal prolyl peptide-catalyzed asymmetric aldol reactions see: (l) Kofoed, J.; Nielsen, J.; Reymend, J.-L. *Biorg. Med. Chem. Lett.* **2003**, *13*, 2445; (m) Martin, H. J.; List, B. *Synlett* **2003**, 1901; (n) Tang, Z.; Yang, Z.-H.; Cun, L.-F.; Gong, L.-Z.; Mi, A.-Q.; Jiang, Y.-Z. *Org. Lett.* **2004**, *6*, 2285; (o) Krattiger, P.; Kovasy, R.; Revell, J. D.; Ivan, S.; Wennemers, H. *Org. Lett.* **2005**, *7*, 1101; For an excellent review on the use of peptides in asymmetric catalysis see: (p) Davie, E. A. C.; Mennen, S. M.; Xu, Y.; Miller, S. J. *Chem. Rev.* **2007**, *107*, 5759.
9. (a) Bahmanyar, S.; Houk, K. N. *J. Am. Chem. Soc.* **2001**, *123*, 12911; (b) Bahmanyar, S.; Houk, K. N. *J. Am. Chem. Soc.* **2001**, *123*, 11273; (c) Bahmanyar, S.; Houk, K. N.; Martin, H. J.; List, B. *J. Am. Chem. Soc.* **2003**, *125*, 2475; (d) Hoang, L.; Bahmanyar, S.; Houk, K. N.; List, B. *J. Am. Chem. Soc.* **2003**, *125*, 16; (e) Clemente, F. R.; Houk, K. N. *Angew. Chem., Int. Ed.* **2004**, *43*, 5766; (f) Rankin, K. N.; Gauld, J. W.; Boyd, R. *J. Phys. Chem. A* **2002**, *106*, 5155; (g) Alleman, C.; Gordillo, R.; Clemente, F. R.; Cheong, P. H.-Y.; Houk, K. N. *Acc. Chem. Res.* **2004**, *37*, 558; (h) Fan, J.-F.; Wu, L.-F.; Tao, F.-M. *Int. J. Quant. Chem.* **2008**, *108*, 66.; For DFT calculations of the acyclic amino acid-catalyzed intramolecular aldol reaction see: (i) Clemente, F. R.; Houk, K. N. *J. Am. Chem. Soc.* **2005**, *127*, 11294.
10. Seebach, D.; Beck, A. K.; Badine, D. M.; Limbach, M.; Eschenmoser, A.; Treasurywala, A. M.; Hobi, R.; Prikoszovich, W.; Linder, B. *Helv. Chem. Acta* **2007**, *90*, 425.
11. Córdova, A.; Zou, W.; Ibrahem, I.; Reyes, E.; Engqvist, M.; Liao, W.-W. *Chem. Commun.* **2005**, 3586.
12. Bassan, A.; Zou, W.; Reyes, E.; Himo, F.; Córdova, A. *Angew. Chem., Int. Ed.* **2005**, *44*, 7028.
13. For selected examples of highly enantioselective intermolecular aldol reactions catalyzed by amino acids with a primary amine functionality see: (a) Jiang, Z.; Liang, Z.; Wu, X.; Lu, Y. *Chem. Commun.* **2006**, 2801; (b) Deng, D.-S.; Cai, J. *Helv. Chim. Acta* **2007**, *90*, 119; (c) Wu, X.; Jian, Z.; Shen, H.-M.; Lu, Y. *Adv. Synth. Catal.* **2007**, *349*, 812; (d) Ramasastry, S. S. V.; Zhang, H.; Tanaka, F.; Barbas, C. F., III. *J. Am. Chem. Soc.* **2007**, *129*, 288; (e) Ramasastry, S. S. V.; Albertshofer, K.; Utsumi, N.; Tanaka, F.; Barbas, C. F., III *Angew. Chem., Int. Ed.* **2007**, *46*, 5572; See also: (f) Amedjkouh, M. *Tetrahedron: Asymmetry* **2005**, *16*, 1411; (g) Limbach, M. *Tetrahedron Lett.* **2006**, *47*, 3843.
14. (a) Zou, W.; Ibrahem, I.; Dziedzic, P.; Sundén, H.; Córdova, A. *Chem. Commun.* **2005**, 4946; (b) Dziedzic, P.; Zou, W.; Hafren, J.; Córdova, A. *Org. Biol. Chem.* **2006**, *4*, 38.
15. (a) Córdova, A.; Zou, W.; Dziedzic, P.; Ibrahem, I.; Reyes, E.; Xu, Y. *Chem. Eur. J.* **2006**, *12*, 5383; (b) Córdova, A.; Zou, W.; Dziedzic, P.; Ibrahem, I.; Reyes, E.; Xu, Y. *Chem. Eur. J.* **2006**, *12*, 5175; (c) Weber, A. L.; Pizzarrello, S. *Proc. Natl. Acad. Sci. U.S.A.* **2006**, *103*, 12713; (d) Tsogoeva, S.; Wei, S. *Tetrahedron: Asymmetry* **2005**, *16*, 1947; (e) Carrea, G.; Ottolina, G.; Lazcano, A.; Pironti, V.; Colonna, S. *Tetrahedron: Asymmetry* **2007**, *18*, 1265.
16. (a) Ledl, Franz; Schleicher, Erwin *Angew. Chem., Int. Ed.* **1990**, *29*, 565; (b) Nursten, H. The Maillard Reaction, Chemistry, Biochemistry and Implications; Royal Society of Chemistry: Cambridge, 2005; (c) Steinhart, H. *Angew. Chem., Int. Ed.* **1999**, *44*, 7503; (d) Somoza, V. *Mol. Nutr. Food Res.* **2005**, *49*, 663.
17. Baynes, J. W.; Monnier, V. M.. *The Maillard Reaction in Ageing*. In *Diabetes and Nutrition; Progress in Clinical and Biological Research*; Alan R. Liss: New York, 1989; Vol. 304.
18. Becke, A. D. *J. Chem. Phys.* **1993**, *98*, 5648.
19. Frisch, M. J.; Trucks, G. W.; Schlegel, H. B.; Scuseria, G. E.; Robb, M. A.; Cheeseman, J. R.; Montgomery, J. A., Jr.; Vreven, T.; Kudin, K. N.; Burant, J. C.; Millam, J. M.; Iyengar, S. S.; Tomasi, J.; Barone, V.; Mennucci, B.; Cossi, M.; Scalmani, G.; Rega, N.; Petersson, G. A.; Nakatsuji, H.; Hada, M.; Ehara, M.; Toyota, K.; Fukuda, R.; Hasegawa, J.; Ishida, M.; Nakajima, T.; Honda, Y.; Kitao, O.; Nakai, H.; Klene, M.; Li, X.; Knox, J. E.; Hratchian, H. P.; Cross, J. B.; Bakken, V.; Adamo, C.; Jaramillo, J.; Gomperts, R.; Stratmann, R. E.; Yazyev, O.; Austin, A. J.; Cammi, R.; Pomelli, C.; Ochterski, J. W.; Ayala, P. Y.; Morokuma, K.; Voth, G. A.; Salvador, P.; Dannenberg, J. J.; Zakrzewski, V. G.; Dapprich, S.; Daniels, A. D.; Strain, M. C.; Farkas, O.; Malick, D. K.; Rabuck, A. D.; Raghavachari, K.; Foresman, J. B.; Ortiz, J. V.; Cui, Q.; Baboul, A. G.; Clifford, S.; Cioslowski, J.; Stefanov, B. B.; Liu, G.; Liashenko, A.; Piskorz, P.; Komaromi, I.; Martin, R. L.; Fox, D. J.; Keith, T.; Al-Laham, M. A.; Peng, C. Y.; Nanayakkara, A.; Challacombe, M.; Gill, P. M. W.; Johnson, B.; Chen, W.; Wong, M. W.; Gonzalez, C.; Pople, J. A. GAUSSIAN *03, Revision D.01*; Gaussian: Wallingford, CT, 2004.
20. Barone, V.; Cossi, M. *J. Phys. Chem. A* **1998**, *102*, 1995.